OVERLAPPING CONTROL VOLUME (OCV) TECHNIQUE FOR SOLUTION OF SHALLOW WATER FLOW EQUATIONS

A Thesis Submitted
in Partial Fulfilment of the Requirements
for the Degree of
MASTER OF TECHNOLOGY

by

NAGAVELLI KARUNAKAR

to the

Department of Civil Engineering
Indian Institute of Technology, Kanpur
September, 1996

CERTIFICATE

This is to certify that the present research work entitled Overlapping Control Volume (OCV) Technique for solution of Shallow Water Flow Equations *has been carried out by* N.KARUNAKAR *under our supervision and it has not been submitted elsewhere for a degree.*

Dr.V. ESWARAN

Associate Professor

Dept. of Mechanical Engineering

Indian Institute of Technology

Kanpur

Dr.B.S. MURTY

Assistant Professor

Dept. of Civil Engineering

Indian Institute of Technology

Kanpur

SEPTEMBER 1996

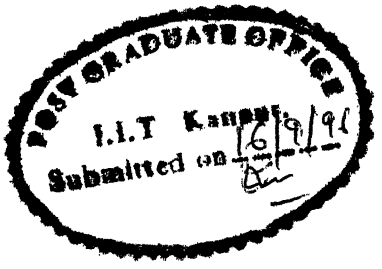

ABSTRACT

The shallow water equations are a set of coupled hyperbolic partial differential equations. As analytical solutions for these equations are not possible for practical cases of open channel flow, they are solved using numerical techniques. *Finite difference* and *finite element* methods have been applied in the past for solving most of the practical cases. However, *Finite Volume Methods* are becoming popular these days because they can be applied to any arbitrary physical domain (like finite element methods) and are easy to implement (unlike finite element methods). In this study, an overlapped control volume (OCV) method is developed for solving the two–dimensional shallow water flow equations. The OCV method is verified by solving steady two–dimensional supercritical flow problems. The test cases solved are channel transitions, the results of which are compared with the solutions obtained by employing a finite difference method.

ACKNOWLEDGEMENTS

I express my profound sense of gratitude to my teachers **Dr. B.S. Murty** and **Dr. V. Eswaran** for suggesting the problem of this thesis and their guidance throughout the work. It was a memorable and an enjoyable experience to work with them.

I am thankful to the staff of the Hydraulics and Water Resources section of Civil Engineering Department especially my teachers Dr. S. Surya Rao, Dr. T. Gangadhariah, Dr. Bithin Datta, Dr. S.Ramasheshan and Dr.K.Subramanya who enforced my foundations in Civil Engineering.

I would like to express my appreciation for the tireless help, innumerable comments and suggestions my friends have given me. My thanks to them are inexpressible. Particularly I would like to thank Bovin, Anand, Ravi, A.Nil, Whyes and Alluri for their help and inspiration which made my stay at Kanpur more enjoyable. The help rendered by my seniors Atul, V.singh , Pranab and Kali worth special mention.

I am , forever, thankful to my parents for their blessings and encouragement received at every juncture, which has helped me to complete my work smoothly.

I wish to express my gratitude to the Ministry of Human Resources Development for the financial support.

Lastly the author is thankful to the Xerox centre of Hall-5 for Photocopying.

- N. Karunakar

TABLE OF CONTENTS

NOTATION

CN	Courant Number
g	acceleration due to gravity, m/s^2
F	Froude number
h	flow depth , m
i	subscript for space node in X direction
j	subscript for space node in Y direction
n	subscript for time level
S_{ox}	channel bottom slope in x-direction
S_{oy}	channel bottom slope in y-direction
S_{fx}	friction slope in x-direction
S_{fy}	friction slope in y-direction
n	Manning's roughness coefficient
t	time
u	flow velocity in x-direction
v	flow velocity in y-direction
V	magnitude of resultant velocity
x	space coordinate
y	space coordinate

Greek letters

α_x	angle between channel and the x-direction
α_y	angle between channel and the y-direction
κ	dissipation constant used in the numerical scheme
Δt	time interval
Δx	distance increment in $x-$ direction
Δy_i	distance increment in $y-$ direction at $x = i$
θ	angle between the wall and the x- axis
δ	inclination of velocity vector at interior node adjacent to boundary
ν	scaling parameter used in artificial viscosity procedure
ω	weighting coefficient

LIST OF FIGURES

Chapter 1

Introduction

Shallow water flow equations are generally used for simulating most of the unsteady open channel flows including flood waves, dambreak flows, flows in estuaries, etc. They are also used often to represent two–dimensional supercritical flows with oblique waves when the shallowness parameter is very small. These equations are a set of coupled hyperbolic partial differential equations . Analytical solutions of these equations are available only for idealized cases; therefore, they are numerically solved for most of the practical applications.

Many numerical methods are available for the solution of the shallow water flow equations. These numerical techniques can be broadly classified into the following types:

1. Finite–difference Methods,

2. Finite–element Methods and

3. Finite–volume Methods.

Historically, Finite–difference methods are the oldest and they are popular even today. Finite–difference methods such as the Priessman scheme, Lax–Wendroff scheme etc. have been traditionally used for solving the one–dimensional shallow water flow equations (Chaudhry, 1993). Fennema and Chaudhry (1990) and Garcia and Kawahita (1986) introduced the MacCormack scheme for solving the

two–dimensional shallow water flow equations. Since then, this method has been extensively used for solving various two–dimensional open–channel flow problems (Jimenez and Chaudhry 1988 , Dammuller et al. 1989 , Bhallamudi and Chaudhry 1992). Fennema and Chaudhry (1990) have also introduced the implicit Beam and Warming method for solving two–dimensional dambreak flow problems. Casulli (1990) developed ADI, semi–implicit and fully implicit splitting Finite–difference methods for solving the two–dimensional shallow water flow equations. Classical second–order accurate finite–difference methods result in dispersive errors when applied to flows with shocks. These dispersive errors manifest in terms of higher–order oscillations near the shock front. Artificial viscosity methods are usually applied to smoothen these higher–order oscillations (Chaudhry, 1993). Recently, Total Variation Diminishing (TVD) schemes (Garcia–Navvarro et al. 1992, Alcrudo et al. 1992) and Essentially Non–Oscillatory (ENO) schemes (Yang et. al. 1993 , Nujic 1995) were introduced for solving the shallow water flow equations. These techniques have a sounder theoretical basis than the artificial viscosity procedures for smoothing the higher–order oscillations. Savic and Holly (1993) developed the modified Godunov method for solving a one–dimensional dambreak flood wave. This method is very useful for solving mixed flow regimes and for flows with strong shocks, without the introduction of artificial viscosity; however, it has not been used for two–dimensional flows.

The main advantage of any finite–difference method is the ease of implementation. They are best suited for one–dimensional applications. However, their application to two–dimensional flows requires approximation at the boundaries if the flow domain is not rectangular. Alternatively, Coordinate transformation techniques may be used for converting the non–rectangular physical domain into a rectangular computational domain (Dammuller et al. 1989, Bhallamudi and Chaudhry 1992, Bellos et al. 1991). Bhallamudi and Chaudhry (1992) used a global transformation of the governing equations while Bellos et al. (1991) used the transformation of equations locally for the non–orthogonal finite–difference grid. This requirement of coordinate transformation makes the application of finite–difference methods difficult in case

of two–dimensional open channel flows in general non–rectangular domains.

Finite–element methods for shallow water flow equations have been developed essentially to overcome the limitations of finite–difference methods for two–dimensional flow in arbitrary domains. Katapodes (1984) developed a dissipative Galerkin scheme for simulating two–dimensional surges and shocks in open channels. The parasitic waves in the vicinity of the discontinuity, commonly present in the classical Galerkin solution, are selectively dissipated in this technique. The method is based on discontinuous weighting functions which introduce upwind effects in the solution. Akanbi and Katapodes (1988) modified the above technique for application to a deforming coordinate system to simulate flood waves propagating on dry bed. The U.S.Army Corps of Engineers (1985) developed a commercial finite–element package for the simulation of unsteady flow in estuaries and bays. This model incorporates a constant eddy viscosity model for turbulence, which helps in dissipating the higher–order oscillations (Chaudhry et al. 1988). Lynch and Gray (1978) and Kawahara and Umetsu (1986) developed finite–element methods for moving boundary problems in river flows. Herrling (1982) developed a finite–element model based on coupling of one– and two–dimensional finite elements for simulating moving boundary problems in estuaries. Leclere et al. (1990) also developed a finite–element model for shallow water flow in estuaries with moving boundaries. This model is based on a fixed spatial mesh with elements becoming dry or wet in a continuous manner. Recently, Galland et al. (1991) developed a commercial software package called TELEMAC for simulation of shallow water flows using a finite–element method. Although finite–element methods can be applied to any irregular flow domains, algorithms based on these techniques are quite complex and require much more computational power than the finite–difference methods for their application to even simple problems.

Finite–volume techniques offer a viable alternative to the finite–element methods for solving the fluid flow problems (Peyret and Taylor 1983). They combine the flexibility of handling the complex geometries, intrinsic to FEM , with the simplicity of FDM. Putti et al. (1990) used a triangular finite–volume tech-

nique for solving the ground water solute transport equation. Verma and Eswaran (1996) developed an Overlapping Control Volume (OCV) method for the solution of two–dimensional Convective–Diffusion equation. Later, Verma et al. (1996) extended this method for simulating two–dimensional solute transport in ground water. Alcrudo and Garcia–Navvarro (1993) introduced a high resolution Godunov–type scheme in finite–volumes for the two–dimensional shallow water flow equations. The method proposed by Alcrudo and Garcia–Navvarro (1993) can be applied to any arbitrary flow domain without the necessity of coordinate transformation.

In this study, an attempt is made to extend the OCV technique developed by Verma and Eswaran (1996) for application to the shallow water flow equations. Unlike the Convective–Diffusive equation solved by Verma and Eswaran (1996) , the shallow water flow equations do not contain the diffusive terms. On the other hand, the complications arise due to the coupled nature of the Continuity and Momentum equations. The proposed method is verified by solving two–dimensional supercritical flow problems in channel transitions. The numerical results obtained obtained using the OCV technique compare satisfactorily with earlier results obtained using the Finite–difference method.

The governing equations for the shallow water flow are presented in Chapter 2 followed by a description of the *OCV* technique in Chapter 3. The *OCV* technique is validated using earlier numerical results obtained by a finite–difference method for channel transitions. Concluding remarks are presented in chapter 5.

Chapter 2

Governing Equations

The two-dimensional shallow water flow equations represent the laws of conservation of mass and momentum for flow in open-channels. These equations are derived from the three-dimensional equations of motion by integrating them over the flow depth. The shallow water equations in cartesian system are written as,

$$U_t + F_x + G_y + S = 0 \tag{2.1}$$

where

$$U = \begin{pmatrix} h \\ hu \\ hv \end{pmatrix}$$

$$F = \begin{pmatrix} uh \\ u^2h + \frac{1}{2}gh^2 \\ uvh \end{pmatrix}$$

$$G = \begin{pmatrix} vh \\ uvh \\ v^2h + \frac{1}{2}gh^2 \end{pmatrix}$$

$$S = \begin{pmatrix} 0 \\ -gh(S_{ox} - S_{fx}) \\ -gh(S_{oy} - S_{fy}) \end{pmatrix}$$

subscripts t, x and y in Eqn 2.1 represent the partial derivatives with respect to time, longitudinal direction and lateral direction, respectively.

In the above equation,

t = time

u = velocity along the longitudinal direction

v = velocity along the lateral direction

h = water depth

g = acceleration due to gravity

S_{ox} = channel slope along the longitudinal direction

S_{oy} = channel slope along the lateral direction

S_{fx} = friction slope along the longitudinal direction

S_{fy} = friction slope along the lateral direction

The bottom slopes are estimated as:

$$S_{ox} = \sin \alpha_x \tag{2.2}$$

$$S_{oy} = \sin \alpha_y \tag{2.3}$$

α_x,α_y are the angles between the bottom of the channel and the longitudinal and lateral direction, respectively.

Friction slopes may be estimated using the Manning's or Chezy's equation.

$$S_{fx} = \frac{n^2 u\sqrt{u^2+v^2}}{h^{4/3}} \tag{2.4}$$

$$S_{fy} = \frac{n^2 v\sqrt{u^2+v^2}}{h^{4/3}} \tag{2.5}$$

where n = Manning's roughness coefficient.

2.1 Assumptions

Shallow water flow equations are based on the following assumptions :

1. The pressure distribution in the vertical direction is assumed to be hydrostatic i.e. the acceleration in the vertical direction is assumed to be negligible.
2. Depth averaged values are used in two-dimensional modelling.
3. Fluid is assumed to be incompressible and the density is same throughout.
4. Velocity distribution is uniform along the depth.
5. The channel bottom is rigid and the bottom slope is small.
6. Only shear stresses due to horizontal velocity components are significant, other turbulence effects are neglected.
7. Frictional resistance is approximated by the Chezy's equation or Manning's equation.

Although shallow water equations are applicable for most of the open–channel flows under subcritical conditions, their application to supercritical flows is limited because of the assumptions 1 and 2. Therefore, these assumptions are discussed briefly in the following paragraphs.

2.1.1 Hydrostatic Pressure distribution:

The assumption of hydrostatic pressure distribution is correct if the streamlines are parallel and straight. As long as high curvatures are not present, the pressure distribution is almost hydrostatic. Ligget (1975) had shown that the assumption is valid as long as a *shallowness parameter* h_0/l_0 (h_0 is water depth and l_0 is characteristic length) is small. Later, Jimenez (1987) concluded that the shallow water theory reasonably represents the supercritical flow if depth to width ratio is of the order of 0.1 and Froude number is not close to unity. The error is of the order of 20% if the depth to width ratio is increased to 0.2. This error is manifested in the wavelength of the resulting wave pattern. The hydrostatic assumption is not valid in the vicinity of the shock and some flow details are lost at the shock location. However the overall results are adequate for engineering purposes (Cunge 1975).

2.1.2 Turbulent effects and Depth averaging:

The depth integration of the three-dimensional equations of motion produce higher order terms known as effective stresses which are not included in the Eq(2.1). Effective stresses constitute laminar viscous stresses, turbulent stresses and stresses due to depth averaging of advective terms. Laminar viscous stresses may be neglected but the other two are important. Consideration of turbulent stresses requires the use of a turbulence closure model which expresses stresses as a function of the main flow variables. Rastogi and Rodi (1978), Puri and Kao (1984) and Leschziner and Rodi (1979) used $K-\epsilon$ models for describing turbulence. Vreugdenhil and Wijbenga (1982) used the constant eddy viscosity concept. However, the above closure models have been tested only for subcritical flows and no information is available for supercritical flows. Inclusion of turbulence effects is beyond the scope of the present study.

Ippen and Harleman (1950) studied the effect of non-uniform velocity distribution and concluded that the effect is negligible.The measurement of velocity across the depth on the front and back side of the jump indicated that the momentum cor-

rection factor ranged from 1.007 at $F_r = 6.3$ to 1.015 at $F_r = 2.0$. It should be noted that though the effect of magnitude variation of velocity may not be significant, yet the variation of velocity across the depth may be significant (Kumar, 1996).

In the present study, it is assumed that the shallow water equations are applicable for supercritical flows also. Their numerical solution is presented in the next chapter.

Chapter 3

Overlapping Control Volume (OCV) Method

The shallow water flow equations are nonlinear hyperbolic partial differential equations and their closed form solutions are available only for very simplified cases. Therefore, they are numerically integrated using a *control volume* approach. An Overlapping Control Volume (OCV) method adapted from Verma and Eswaran (1996) and Verma et al. (1996) is used for this purpose. However, the flux calculation at the control surface of the control volume is different in the present application. Also, the partial discretization for time is done using a MacCormack like scheme (MacCormack, 1969). The proposed scheme is an explicit, two–step predictor–corrector scheme which is second order accurate, in time and space, and is capable of capturing shocks without isolating them. The method is applicable on non–orthogonal grids.

3.1 Finite–Volume Formulation

The physical domain over which the solution is sought is discretized into a structured non–orthogonal grid as shown in Fig 3.1a . A Control Volume as shown in Fig 3.1b is considered. The Control Volume is labelled by the index of the control node i.e., as (i,j). This type of Control Volume uses the grid point coordinates to form the Control

Volumes. Therefore, unlike in the usual Control Volume approach, it does not involve the determination for any of the intermediate points. However, the adjacent Control Volumes will overlap each other: hence the name "Overlapping Control Volume" technique. The governing equation for the control volume is obtained by integrating the Eq.(2.1) over the control volume and applying the Gauss divergence theorem.

$$\int_{cv}\int \frac{\partial U}{\partial t} dA + \oint_{cs} (Fn_x + Gn_y) dl = \int_{cv}\int S dA \tag{3.1}$$

where, dl is an elemental length on the boundary (Control Surface) of the Control Volume, n_x and n_y are the direction cosines of the local outward unit vector on the boundary in x and y directions, respectively, and dA is the elemental area of the Control Volume.

3.2 Solution of Governing Equation

Equation (3.1) is solved for any control volume (i,j) using an explicit predictor–corrector approach. Discretization of Eq (3.1) for an explicit solution for time level $t + \Delta t$ is explained in the following sections.

3.2.1 Predictor Step

Equation (3.1) is partially discretized in the predictor step as,

$$\frac{U^*_{i,j} - U^n_{i,j}}{\Delta t} A_s = S^n_{i,j} A_s - (Flux)^n \tag{3.2}$$

where

$$(Flux)^n = \int_{cs} (Fn_x + Gn_y) dl \tag{3.3}$$

As is the area of the Control Volume and Δt is the computational time step. Subscript (i,j) indicates the Control Volume and the superscripts $*$ and n in Eqs. (3.2) and (3.3) denote the evaluation of the terms at the predictor level and the time

level "t" , respectively. The area of the control volume (A_s) is calculated using the formula

$$\begin{aligned} A_s &= 0.5[(x_{i,j+1} - x_{i+1,j})(y_{i,j-1} - y_{i+1,j}) - (x_{i,j-1} - x_{i+1,j})(y_{i,j+1} - y_{i+1,j}) \\ &\quad +(x_{i,j-1} - x_{i-1,j})(y_{i,j+1} - y_{i-1,j}) - (x_{i,j+1} - x_{i-1,j})(y_{i,j-1} - y_{i-1,j})] \end{aligned}$$

where $x_{i,j+1}, y_{i,j+1}$ etc., are the coordinates of the neighbouring points shown in Fig. 3.1b. The contour integration for the term $Flux$ in Eq.(3.2) is counter–clockwise. Discretization of this term is explained in detail below.

3.2.2 Continuity Equation:

The U variable in Eq.(3.2) is h for the continuity equation. For determining the predicted flow depth, h^*, $Flux$ is discretized as

$$\begin{aligned} Flux &= \sum_{k=1}^{4} h^{(k)} \left(u^{(k)}\Delta y^{(k)} - v^{(k)}\Delta x^{(k)}\right) \\ &= \sum_{k=1}^{4} h^{(k)} J^{(k)} \end{aligned} \tag{3.4}$$

where the superscript (k) refers to the edges of the control volume(see Fig 3.1b). For the edge (k), k=1,2 and 3, the approximation used is

$$u^{(k)} = 0.5(u_k + u_{k+1}) \tag{3.5}$$

$$v^{(k)} = 0.5(v_k + v_{k+1}) \tag{3.6}$$

$$\Delta y^{(k)} = (y_{k+1} - y_k) \tag{3.7}$$

$$\Delta x^{(k)} = (x_{k+1} - x_k) \tag{3.8}$$

where the subscript k refers to the grid point number as shown in Fig 3.1 b. For k=4, u_{k+1}, x_{k+1} etc. are replaced by u_1, x_1 respectively, in the above equations.

To incorporate upwinding, $h^{(k)}$ in Eq.(3.4) is approximated at the mid–point of control–surface k by interpolation within the upwind control volume adjacent to the surface. For example, referring to Fig. 3.1 b , if the flow is entering the

control volume (i,j) across face 1 ,i.e., $J^{(1)}$ is negative, then $h^{(1)}$ is approximated by interpolation within the control volume for node $(i-1, j-1)$. The values at the grid points constituting the control volume $(i-1, j-1)$ are used for determining $h^{(1)}$. On the other hand, if $J^{(1)}$ is positive, the values at the grid points of the control volume (i, j) are used to obtain $h^{(1)}$. The interpolation scheme to obtain the $h^{(k)}$ value at the face k is explained below.

Consider face 3 of the control volume (i, j) shown in Fig 3.2. $h^{(3)}$ at the mid–point of face 3 is obtained using the grid–point values of h for the control volume (i, j) if $J^{(3)}$ is positive. For this purpose, Verma and Eswaran (1996) and Verma et al. (1996) suggested an interpolation scheme based on finite–element type shape functions. However, it was found during the code development that such an interpolation scheme did not give good results in case of shallow water equations. This was particularly so when a MacCormack type discretization was used for the time stepping. Therefore the following procedure was adopted in the present study.

If the velocity vector at face 3 (obtained as the result of $u^{(3)}$ and $v^{(3)}$) cuts

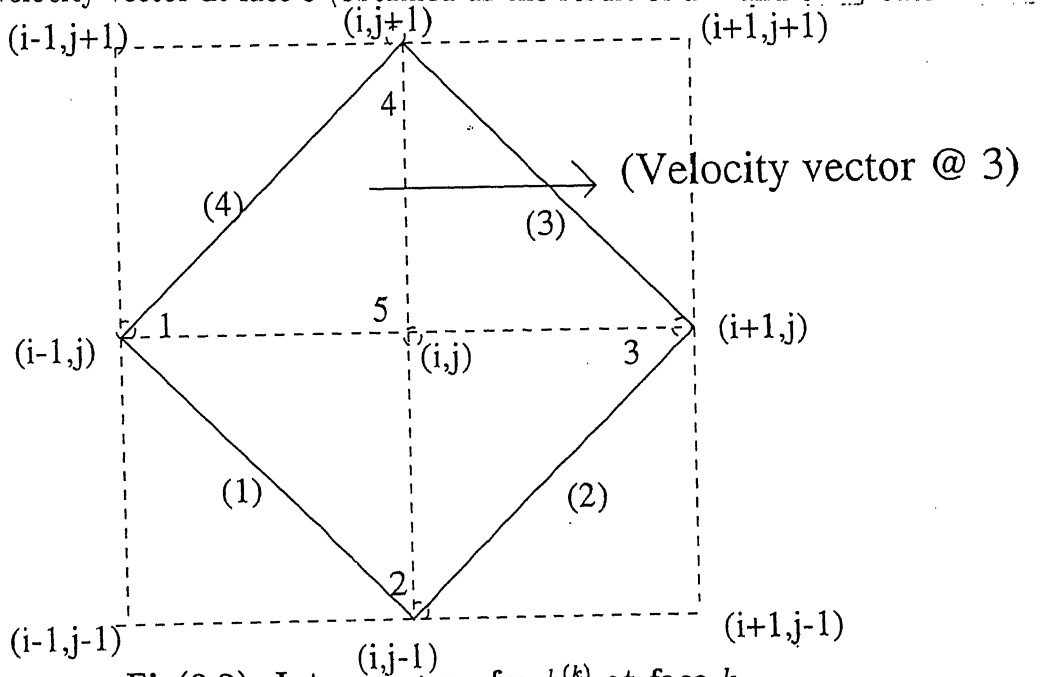

Fig(3.2): Interpolation for $h^{(k)}$ at face k

the diagonal joining the grid points 4 and 5 (see Fig 3.2), then $h^{(3)}$ is obtained as

$$h^{(3)} = 0.5(h_4 + h_5) \tag{3.9}$$

If the velocity vector at face 3 cuts the diagonal joining the grid points 3 and 5, then $h^{(3)}$ is obtained as

$$h^{(3)} = 0.5(h_3 + h_5) \tag{3.10}$$

Similar procedure is adopted while determining $h^{(1)}$, $h^{(2)}$ and $h^{(4)}$. Substitution of Eqs (3.4)–(3.10) in Eq.(3.2) results in an explicit equation for the solution of predicted flow depth at (i,j) i.e., $h^{\star}_{i,j}$, since all other terms are evaluated at time level "t" at which the solution is known.

3.2.3 Momentum Equation

The U variable in Eq. 3.2 is (uh) for solving the momentum equation in x–direction. For determining the predicted value of $uh^{\star}$, the $Flux$ term is discretized as

$$\begin{aligned} Flux &= \sum_{k=1}^{4}(uh)^{(k)}[u^{(k)}\delta y^{(k)} - v^{(k)}\Delta x^{(k)}] + \sum_{k=1}^{4} gh^{(k)}[\frac{(h')^{(k)}}{2}\Delta y^{(k)}] \\ &= \sum_{k=1}^{4}(uh)^{(k)}[J^{(k)}] + \sum_{k=1}^{4} gh^{(k)}[\frac{(h')^{(k)}\Delta y^{(k)}}{2}] \end{aligned} \tag{3.11}$$

in which, the definition of superscripts is same as before. The approximation for $u^{(k)}$, $v^{(k)}$, $\Delta x^{(k)}$, $\Delta y^{(k)}$ and $h^{(k)}$ are also same as described for the continuity equation. The term $h'^{(k)}$ is obtained as

$$h'^{(k)} = 0.5(h_k + h_{k+1}) \tag{3.12}$$

for k= 1,2 and 3. $h'^{(4)}$ is obtained by replacing h_{k+1} by h_1 in Eq.(3.12). The upwinding and the interpolation scheme to obtain $(uh)^{(k)}$ at the mid–point of the face k are similar to the procedures described for obtaining $h^{(k)}$ in the continuity equation. Substitution of Eqs. (3.5)–(3.12) in Eq.(3.2) results in an explicit equation for the solution of $(uh)^{\star}_{i,j}$ since all other terms are evaluated at the time level t. The predicted value of x–velocity at (i,j) i.e., $u^{\star}_{i,j}$ can then be determined as,

$$u^{\star}_{i,j} = \frac{(uh)^{\star}_{i,j}}{h^{\star}_{i,j}} \tag{3.13}$$

The procedure for determining $v^{\star}_{i,j}$ using the momentum equation in y–direction is similar to the procedure described for determining $u^{\star}_{i,j}$. The $Flux$ term in this case is discretized as

$$\begin{aligned} Flux &= \sum_{k=1}^{4}(vh)^{(k)}[u^{(k)}\delta y^{(k)} - v^{(k)}\Delta x^{(k)}] - \sum_{k=1}^{4} gh^{(k)}[\frac{(h')^{(k)}}{2}\Delta x^{(k)}] \\ &= \sum_{k=1}^{4}(vh)^{(k)}[J^{(k)}] - \sum_{k=1}^{4} gh^{(k)}[\frac{(h')^{(k)}\Delta x^{(k)}}{2}] \end{aligned} \tag{3.14}$$

3.2.4 Corrector step

The predicted values of depth and velocities i.e. $h^{\star}$, $u^{\star}$ and $v^{\star}$ are used in a corrector step to obtain the corrected values of depth and velocities. Superscript $\star\star$ in the following equations represents the values of h, u and v at the end of the corrector step. Eq. (3.1) is partially discretized in the corrector step as

$$\frac{U^{\star\star}_{i,j} - U^{n}_{i,j}}{\Delta t} A_s = S^{\star}_{i,j} A_s - (Flux)^{\star} \tag{3.15}$$

The discretization of the term $Flux^{\star}$ in Eq.(3.15) is similar to the discretization of the term $Flux^{n}$ in Eq.(3.2) except that downwinding is incorporated instead of the upwinding and predicted values are used instead of the values at time level t. This means that $h^{(k)}$, $(uh)^{(k)}$ and $(vh)^{(k)}$ in Eqs. (3.4), (3.11) and (3.14) are approximated at the mid–point of the control–surface k by interpolation within the downwind control volume adjacent to the surface. For example, referring to Fig. 3.1b, if the flow is entering the control volume (i,j) across face 1 , i.e. $J^{(1)}$ is negative, then $h^{(1)}$, $(uh)^{(1)}$ and $(vh)^{(1)}$ are approximated by interpolation within the control volume for node (i,j). The predicted values at the grid points constituting the control volume (i,j) are used for determining $h^{(1)}$, $(uh)^{(1)}$ and $(vh)^{(1)}$. Rest of the procedure to determine $h^{\star\star}$, $u^{\star\star}$ and $v^{\star\star}$ is same as that described for the predictor step in the previous section.

3.2.5 Solution at the time level $t + \Delta t$

The values of flow depth and velocity at the time level $t+\Delta t$ are obtained by taking an average of the predicted and the corrected values of U.

$$U_{i,j}^{n+1} = 0.5(U_{i,j}^{*} + U_{i,j}^{**}) \tag{3.16}$$

3.3 Initial and Boundary Conditions

To start the unsteady state computations, the values of three primary variables h, u and v at $time = 0$ are specified at all the grid points. In the present application of the proposed numerical scheme, unsteady flow equations are used in a false transient approach to determine the steady state solutions. In the false transient approach, uniform velocity and uniform flow depth equal to the upstream boundary values are specified at all the nodes as the initial condition. It should be noted that any arbitrary values may be assumed as the initial condition since only the final steady state solution is of interest.

The determination of u, v and h during the unsteady computations requires the application of the boundary conditions at the boundaries of the flow domain. Hyperbolic equations are sensitive to the numerical treatment of the boundary conditions because errors introduced at the boundaries propagate and reflect throughout the domain and in many cases the instability may result (Anderson et. al. 1984). Three type of boundaries are encountered in the present study:

1. The open (flow) boundaries.

2. The symmetry boundary.

3. Solid side wall boundary.

3.3.1 Flow Boundaries

Inflow and outflow boundaries are open boundaries where flow can enter or leave the computational domain. The specification of boundary conditions depends on whether the flow is subcritical or supercritical. (Stoker, Verbroom et al.). In the present study, the proposed numerical scheme is applied for solving the two-dimensional supercritical flow. Therefore, three boundary conditions are to be specified at the inflow boundary and none at the outflow boundary. In the present study u, v and h are specified at the inflow boundary of the channel. These quantities at the downstream nodes are obtained by extrapolation from the already computed values at the interior nodes. Since the flow is supercritical, the extrapolation affects only a few points at the downstream end and the errors will not propagate upstream.

3.3.2 symmetry boundary

Reflection procedure is implemented at a symmetry boundary(Roache 1972). All non-conservative flow variables other than the normal velocity (u and h) are specified as even functions with respect to the symmetry line while the normal velocity is specified as an odd function so that the average normal velocity at the symmetry boundary is zero. The reflection technique is exact for a straight symmetry line.

3.3.3 Solid Side wall boundary

Since all the stresses other than the bottom stresses are neglected, the slip condition is the proper boundary condition for the solid boundaries. The basic requirement at a solid wall is that no flow should take place normal to the boundary, which is expressed as

$$\tan\theta = \frac{v}{u} \tag{3.17}$$

where θ is the angle between the wall and the x-axis. Therefore , the resultant velocity at a solid wall is tangent to it. Abbott(1971), Roache(1972)and Anderson et al.(1984) discussed several wall boundary techniques. Jimenez(1987) tested several techniques for the case of steady supercritical flow. The reflection procedure is used

in the present study. It should be noted that this procedure for the solid side walls is only approximate. Implementation of the reflection procedure depends on the sign and the magnitude of the values of θ and δ (δ = inclination of the velocity vector at the interior node adjacent to the boundary).

One of the possible scenarios for the case of channel expansion is explained here for illustration. Similar results can be obtained for other cases. Referring to Fig. (3.3) , the flow depth and the magnitude of resultant velocity at the imaginary reflection point are same as that of their values at the corresponding interior grid point. The direction of the flow velocity is determined such that the normal velocity at the wall is zero (Bhallamudi and Chaudhry,1992).

$$h_{fic} = h_{int} \tag{3.18}$$

$$V_{fic} = V_{int} \tag{3.19}$$

where subcript fic refers to the values at the "fictitious" reflection point and subscript int refers to the values at the interior point adjacent to the wall. If θ is the angle between the wall and the x–axis and δ is the angle between the resultant velocity at the interior point and the x– axis ,then, the velocity components u_{fic} and v_{fic} at the reflection point are given by ,

$$V_{int} = \sqrt{u_{int}^2 + v_{int}^2} \tag{3.20}$$

$$u_{fic} = V_{int} \cos(2\theta - \delta) \tag{3.21}$$

$$v_{fic} = V_{int} \sin(2\theta - \delta) \tag{3.22}$$

3.4 Stability Condition

The proposed numerical scheme uses an explicit time stepping procedure. Therefore, Courant-Friedrichs-Lewy(CFL) condition has to be satisfied for numerical stability. Shallow water equations are nonlinear and hence this condition, though not strictly applicable, is used as a guideline. The condition for two dimensional flows is given by (Roache 1972),

$$\Delta t \leq \frac{CN}{V+\sqrt{gh}} \frac{1}{\sqrt{\frac{1}{\Delta x^2}+\frac{1}{\Delta y^2}}} \tag{3.23}$$

where V is the velocity at the grid point and CN is the courant number. CN should be less than *one* for obtaining numerically stable results.

3.5 Artificial Viscosity

The proposed scheme is second order accurate in both space and time and will result in dispersive errors. These dispersive errors cause high–frequency oscillations near steep gradients. To smoothen these oscillations, a procedure developed by Jameson et al. (1981) is employed. This procedure smoothens regions of large gradients while leaving smooth areas relatively undisturbed. The values of the variables at the new time computed by the proposed method are modified using the following algorithm. A scaling parameter ν is first determined based on the water level variation.

$$\nu_{x_{i,j}} = \frac{|(h_{i+1,j} - 2h_{i,j} + h_{i-1,j})|}{|h_{i+1,j}| + |2h_{i,j}| + |h_{i-1,j}|} \tag{3.24}$$

$$\nu_{y_{i,j}} = \frac{|(h_{i,j+1} - 2h_{i,j} + h_{i,j-1})|}{|h_{i,j+1}| + |2h_{i,j}| + |h_{i,j-1}|} \tag{3.25}$$

At points where $h_{i,j-1}$ does not exist,

$$\nu_{y_{i,j}} = \frac{|(h_{i,j+1} - h_{i,j})|}{|h_{i,j+1}| + |h_{i,j}|} \tag{3.26}$$

and where $h_{i,j+1}$ does not exist,

$$\nu_{y_{i,j}} = \frac{|(h_{i,j-1} - h_{i,j})|}{|h_{i,j-1}| + |h_{i,j}|} \tag{3.27}$$

The scaling parameter ν and the dissipation constant κ (the value of which is assigned empirically) are used to establish the level of artificial dissipation to be introduced.

$$\varepsilon_{x_{i-\frac{1}{2},j}} = \kappa \max(\nu_{x_{i-1,j}}, \nu_{x_{i,j}}) \tag{3.28}$$

$$\varepsilon_{y_{i,j-\frac{1}{2}}} = \kappa \max(\nu_{y_{i,j-1}}, \nu_{y_{i,j}}) \tag{3.29}$$

The corrected values of any time–stepped variable $f(= h, uh, etc.)$ at the new time step are then given by the following equation :

$$\begin{aligned}(f_{i,j}^{k+1})_{mod} = f_{i,j}^{k+1} \quad + \quad & [\varepsilon_{x_{i+\frac{1}{2},j}}(f_{i+1,j}^{k+1} - f_{i,j}^{k+1}) - \varepsilon_{x_{i-\frac{1}{2},j}}(f_{i,j}^{k+1} - f_{i-1,j}^{k+1})] \\ & + [\varepsilon_{y_{i,j+\frac{1}{2}}}(f_{i,j+1}^{k+1} - f_{i,j}^{k+1}) - \varepsilon_{y_{i,j-\frac{1}{2}}}(f_{i,j}^{k+1} - f_{i,j-1}^{k+1})] \end{aligned} \tag{3.30}$$

where subscript *mod* refers to the modified value of f. The dissipation constant κ is used to regulate the amount of dissipation. This procedure is equivalent to adding second–order dissipative terms to the original governing equations. The actual numerical eddy viscosity coefficient is of the order of $\kappa\nu_x\Delta x^2/\Delta t$ (in x–direction). This indicates that the influence of κ on the results depends upon the gradients in the flow depth as well as grid size. The influence of κ in smooth regions is minimal since ν tends to zero in such cases. The value of κ is chosen such that it is as small as possible but at the same time smoothens the high–frequency oscillations. The presence of the friction term , which is dissipative in nature, tends to inhibit the oscillations. Therefore, a smaller value of κ is taken in those situations.

3.6 Weighted Upwind–Downwind Method

In the proposed method, first–order upwinding is used in the predictor part while first–order downwinding is used in the corrector part. Also, equal weightages are assigned to both predicted and corrected values while determining the values of the variables at the new time level (see Eq. 3.16). Assigning of equal weightages to upwinding and downwinding results in second–order accuracy and the consequent dispersive errors. Therefore, in the present study, it is proposed to determine the values at the time level $t + \Delta t$ as

$$U_{i,j}^{n+1} = \frac{\omega U_{i,j}^{*} + (2 - \omega)U_{i,j}^{**}}{2.0} \tag{3.31}$$

where ω is a weighting coefficient whose value is greater than one but less two. ω=1 results in the second–order accurate scheme while $\omega = 2$ results in a first–order upwind scheme without dispersive errors. In such a case, smoothening of the solution by Jameson's method as described in the previous section may not be necessary. If we choose $1 < \omega < 2$, we can optimise the value of ω , so that we minimize the loss of accuracy while at the same time removing dispersive errors.

3.7 closure

In this chapter, details of the Overlapping Control Volume (OCV) method for the solution of the shallow water flow equations are presented. The implementation of the boundary conditions using the reflection technique is discussed. A weightage upwind–downwind method is proposed to obtain less than second–order accurate solutions, but which have minimum dispersive errors. The proposed scheme is verified in the next chapter.

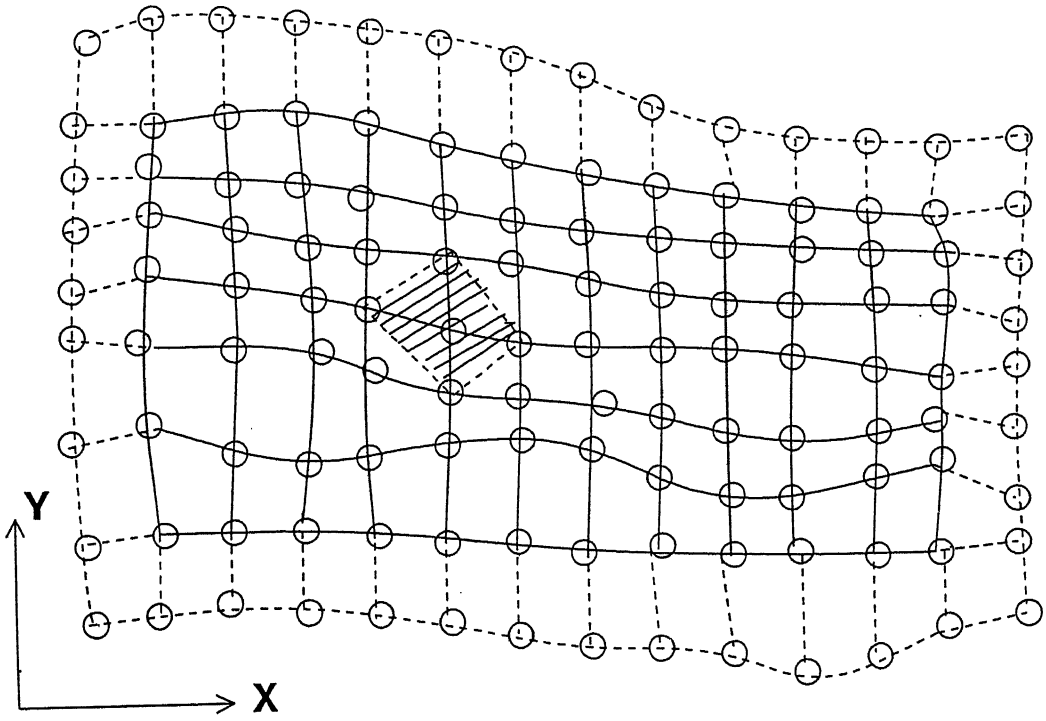

(a)

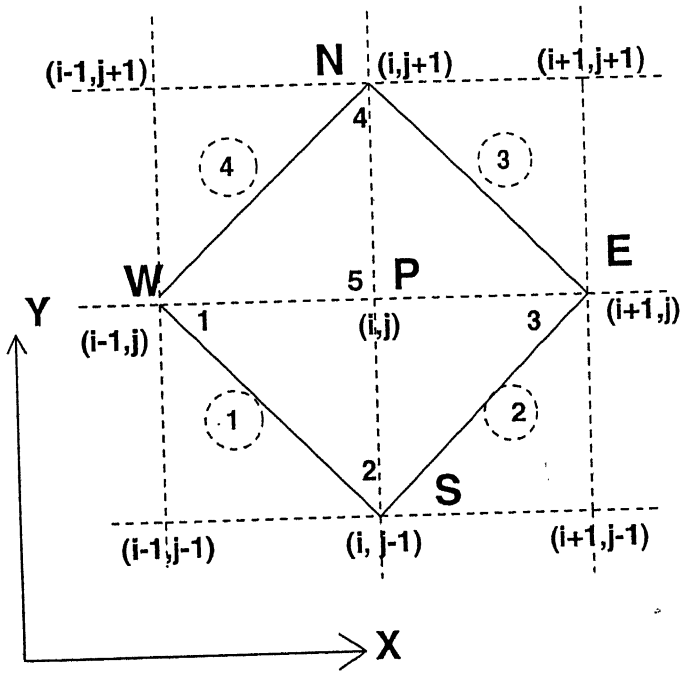

(b)

Fig 3.1 Finite - Volume Grid

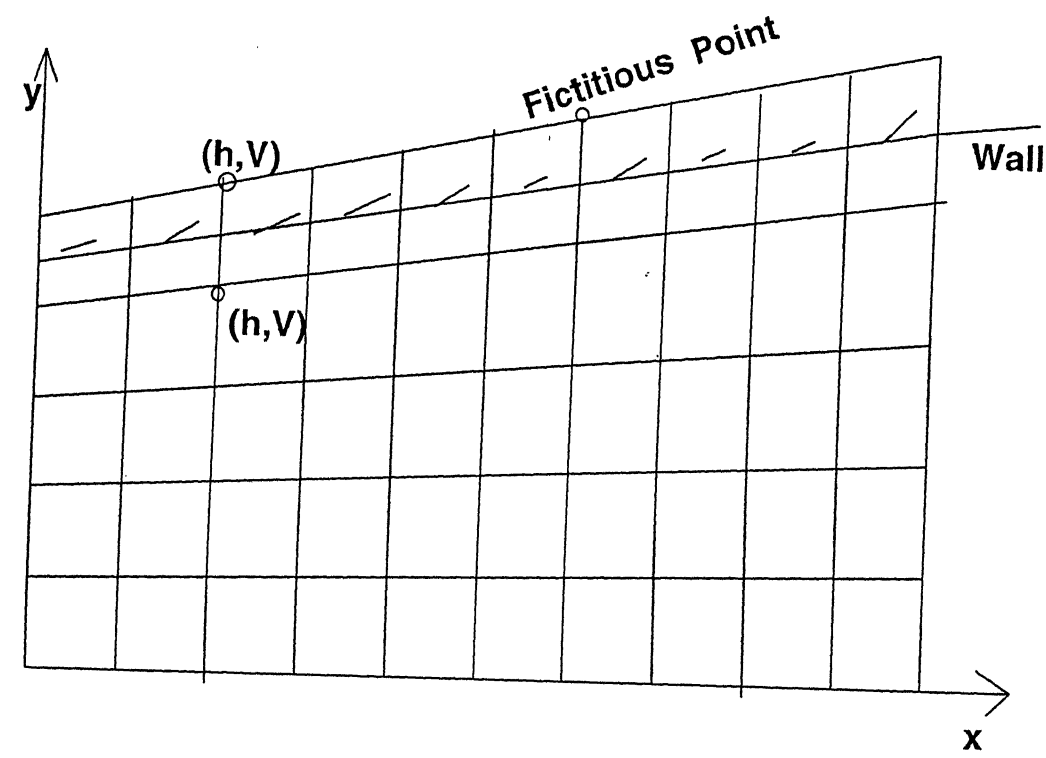

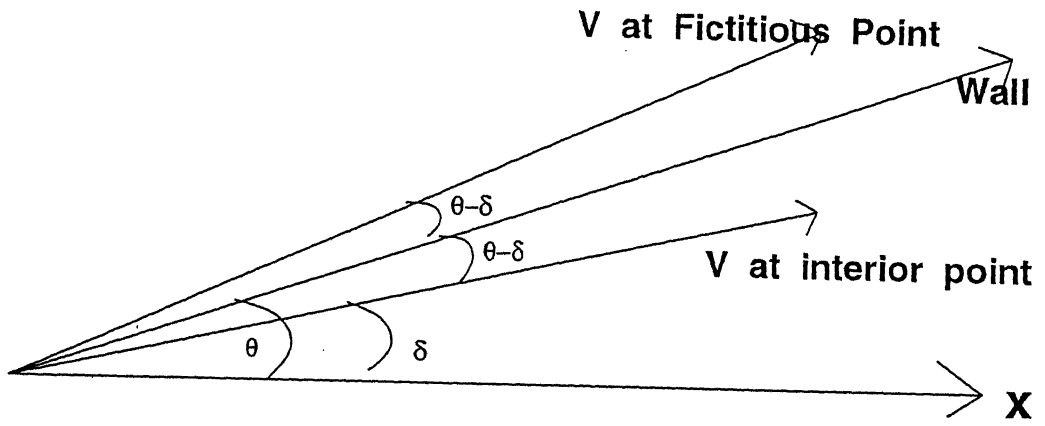

Fig 3.3 Reflection procedure for a Wall (solid side wall Boundary)

Chapter 4

Verification of the Model

The numerical technique presented in chapter 3 is verified here by applying the technique to obtain the flow profiles in channel transitions. The numerical results are compared with the corresponding results obtained by Bhallamudi and Chaudhry (1992) with a finite difference method. The numerical results are also compared with the laboratory test data available in the literature. Results for the two test cases are discussed in the following sections.

4.1 Symmetrical Straight Wall Contraction

Coles and Shintaku(Ippen et al. 1951) tested supercritical flow in the contraction shown in Fig.4.1. The upstream depth,h_0 , was 0.0305m and the upstream Froude number,F_0 , was equal to 4.0. These test results were simulated in the present study using a grid Δx = 0.02415m and 12 grid divisions in the y–direction. The dissipation constant κ =0.8 and the Courant number(C_N) was equal to 0.80. It was assumed that the friction and bottom slopes were equal to zero. A uniform depth of 0.0305m, streamwise velocity of 2.188 m/s and zero transverse velocity were specified at every grid point as the initial conditions. During the computations, h, u and v at the upstream section were specified as 0.0305m , 2.188m/s and zero, respectively, to simulate the upstream boundary conditions. No condition was specified at the downstream boundary; however, values of the variables at the downstream end were

extrapolated from the interior points. The flow conditions were computed upto a time when the flow became steady.

Fig.4.2 and Fig.4.3 show the comparison between the results obtained using the OCV technique and the results obtained by employing finite difference method (Bhallamudi and Chaudhry, 1992). Also shown in these figures are the measured values obtained by Coles and Shintaku (Ippen et al. 1951). Fig. 4.2 shows the water surface profile along the centerline while Fig. 4.3 shows the water surface profile along the wall. It is evident from these figures that the agreement between the results obtained using the OCV technique and the results obtained using the finite difference method (Bhallamudi and Chaudhry, 1992) is very good. Therefore, it can be concluded that the OCV technique is as good as the finite–difference method for solving the shallow water flow equations. The OCV technique, moreover, does not require a coordinate transformation when applied to non–rectangular physical domains. This is the main advantage of the OCV technique. The agreement between the experimental and computed water surface profiles is good along the walls and at the centerline where the flows are smooth. This is not the case for the centerline profile in the vicinity of strong shocks. However, the computed results may be confidently used for engineering applications e.g. for selecting wall height (Bhallamudi and Chaudhry, 1992) .

To investigate the effect of artificial viscosity on the computed results, the OCV technique is applied to the present case with κ values of 0.4 and 0.8 . The computed water surface profiles along the centerline for these two runs are shown in Fig 4.4 . It is clear from this figure that a two–fold increase in the artificial viscosity term changes the results only slightly in the vicinity of the shock, but does not affect the results at other sections.

To investigate the effect of grid size on the computed results, the OCV technique is applied to the present case by taking a grid size which is two times the grid size taken earlier. The dissipation constant κ for this run is equal to 0.8 . The results along the centerline for this case are shown in Fig. 4.5 . It can be seen from Fig. 4.5 that a two–fold increase in the grid size smears the shock and also reduces the

maximum height slightly. As noted earlier in Chapter–3 , the amount of dissipation introduced by the artificial viscosity procedure increases with an increase in grid size, and hence the smearing of shock.

4.2 Super critical flow in a gradual expansion

Rouse et al.(1951) suggested the following equation for the boundaries of a gradual expansion (Fig 4.6)

$$\frac{2B_x}{B_0} = (\frac{x}{B_0 F_0})^{1.5} + 1 \tag{4.1}$$

A transition with the above boundaries is gradual enough so that it reduces the short wave effects and prevents flow seperation. The OCV technique was used to simulate supercritical flow in an expansion with the upstream Froude number, F_0= 2.0 and the upstream depth to width ratio, h_0/b_0= 0.25. Steady supercritical flow conditions at the upstream section were specified at every grid point as the initial condition. The values of h, u and v specified at upstream section as the boundary conditions were 0.0305m, 2.288m/s and zero respectively. Manning's n was specified as 0.012 and the bottom slope was zero. Computations were performed with a Courant number equal to 0.90, dissipation constant κ=0.3 , and a grid size of, Δx=0.01525m. Seven grid divisions are taken in y- direction . Fig. 4.7 and Fig. 4.8 show the comparison between the results obtained by the OCV method and those obtained by employing the finite difference method (Bhallamudi and Chaudhry, 1992) . Fig 4.7 shows the water surface profile along the centerline while Fig. 4.8 shows the results along the wall. Experimental data obtained by Rouse et al. (1951) are also shown in these figures. It can be seen from these figures that the agreement between the results obtained using the OCV technique and the results obtained using the finite–difference method (Bhallamudi and Chaudhry, 1992) is good. The numerical results also match with the experimental data (Rouse et al. 1951) satisfactorily. These results confirm that the OCV technique is as good as the finite–difference method for solving the shallow water flow equations. The numerical results matched satisfactorily with the experimental results because the assumption

of hydrostatic pressure distribution is valid in this case. It can be seen that, unlike in a contraction, the water surface profile in Rouse's expansion is very smooth.

The OCV technique with weighted upwinding–downwinding (without the use of artificial viscosity procedure) is also used to simulate the experiments in the Rouse's expansion. The computed water surface profiles along the centerline and along the wall for this case are presented in Figs. 4.9 and 4.10 , respectively. The value of the weightage parameter, ω was equal to 1.31 in these runs. It is evident from these figures that the weighted upwind-downwind method gives as good results as the finite–difference method. However, it should be mentioned here that the results obtained using the weighted upwind–downwind method are very sensitive to the value of ω. Large values of ω results in excessive numerical dissipation. The ω value was chosen such that it is as close to unity as possible while at the same time eliminating higher order numerical oscillations. It should also be noted here that satisfactory results could not be obtained for the case of contraction when the weighted upwind–downwind method was used. Further studies are needed to improve the accuracy of this technique.

The effect of κ on the computed results for the expansion was investigated by taking two different values of κ equal to 0.3 and 0.6 . The results for the centerline and the wall are presented in Figs. 4.11 and 4.12 , respectively. It can be observed that a two–fold increase in the artificial viscosity does not affect the results significantly.

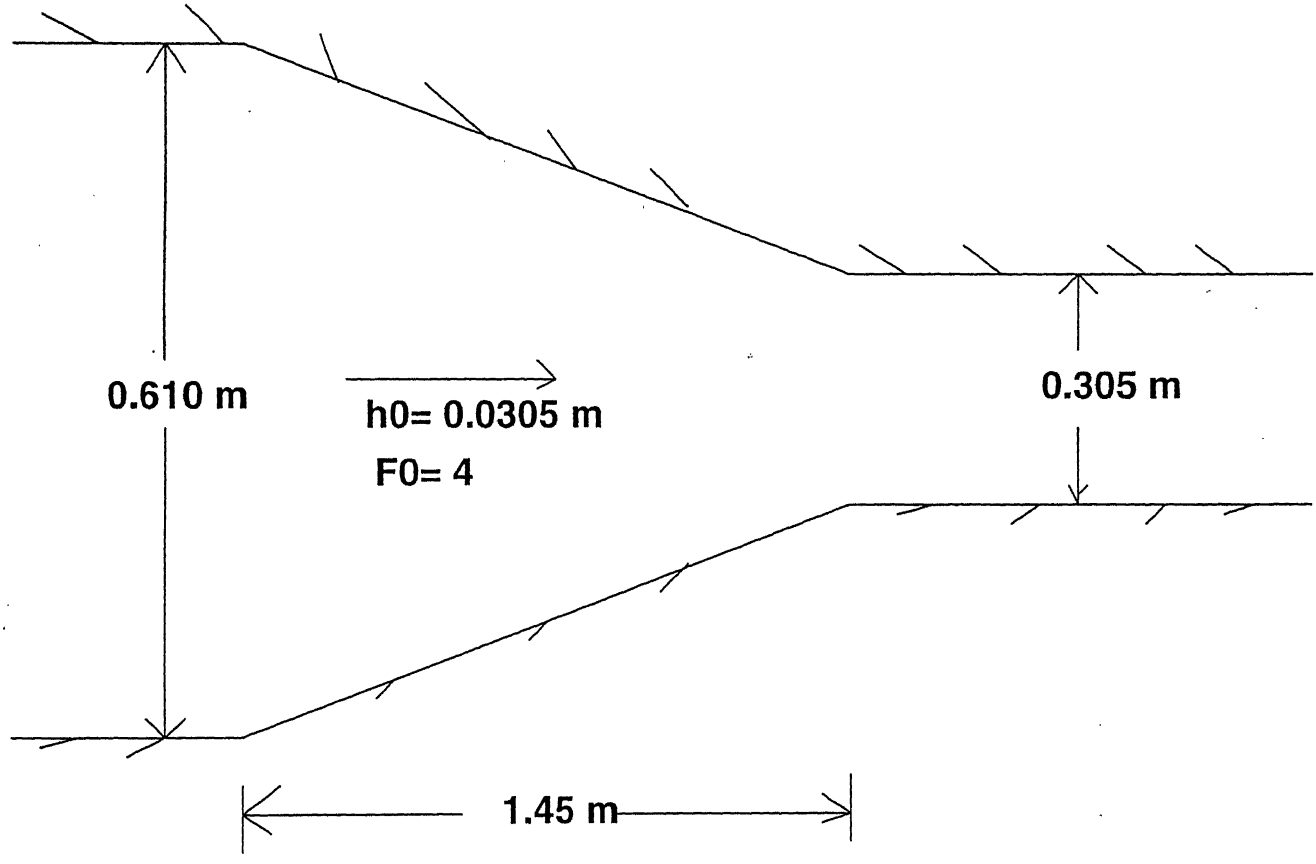

Fig 4.1 Straight Wall Contraction

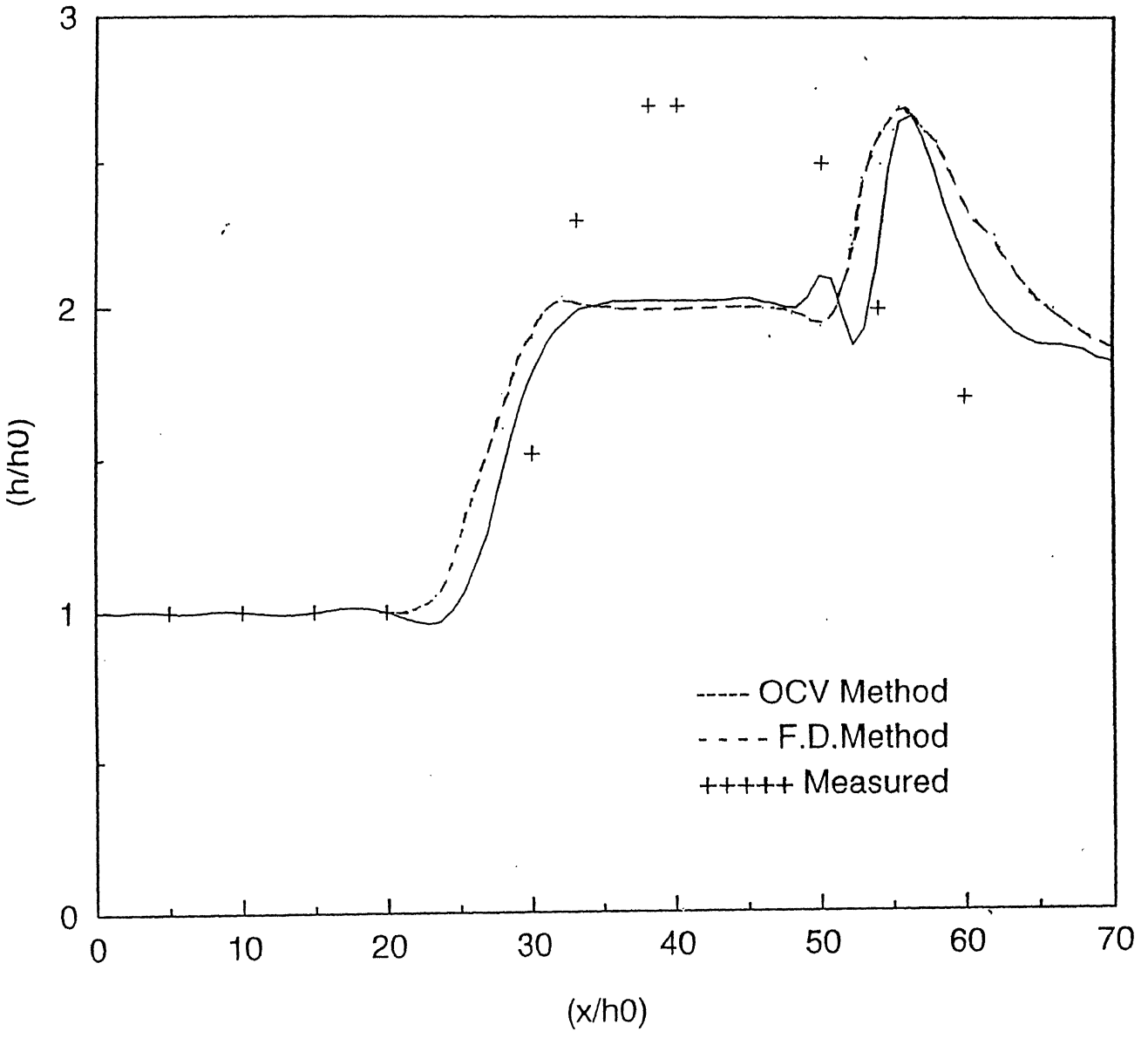

Fig 4.2 Water surface profiles along the Centerline of Contraction of Fig 4.1

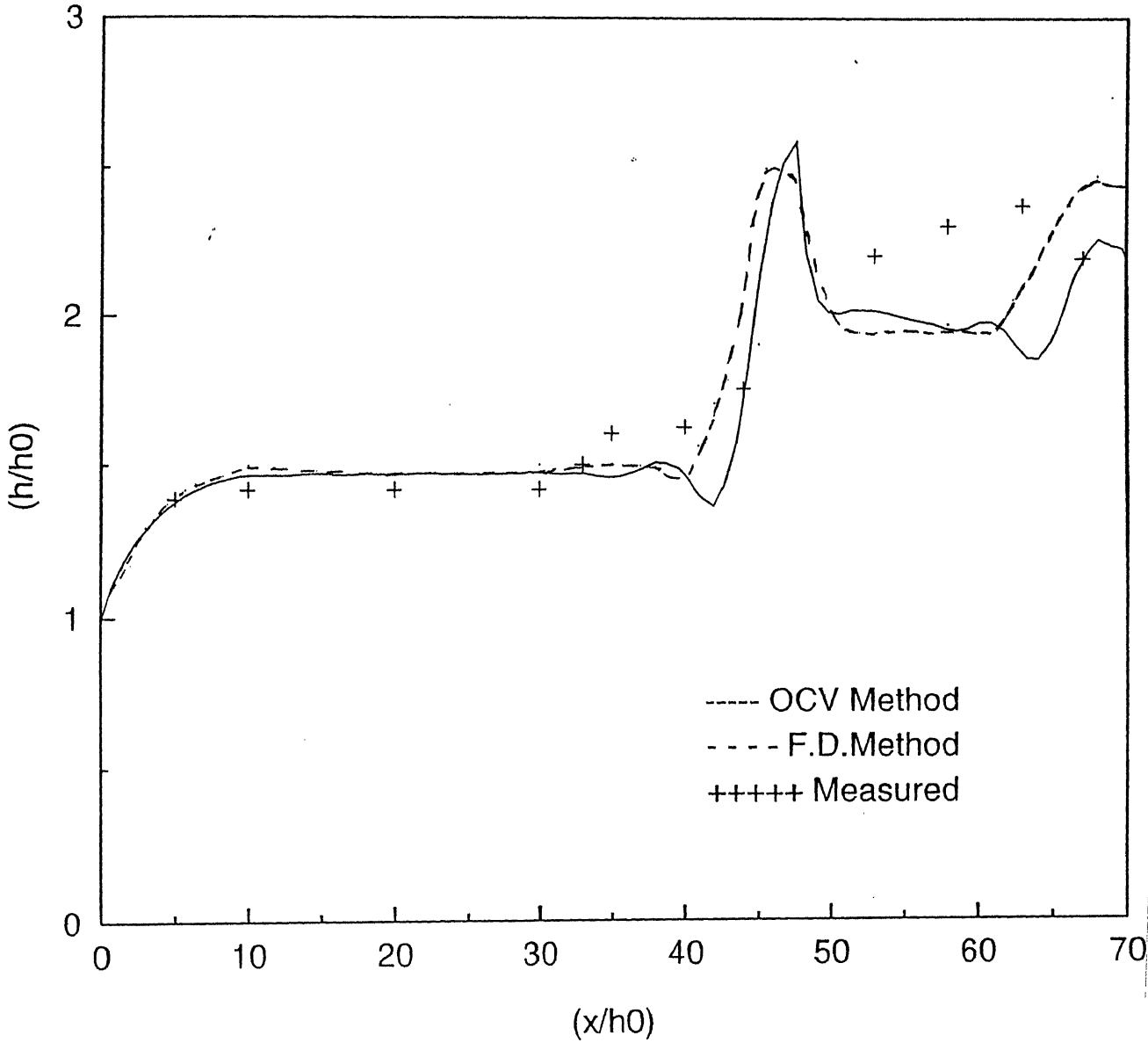

Fig 4.3 Water surface profile along the wall for Contraction of Fig 4.1

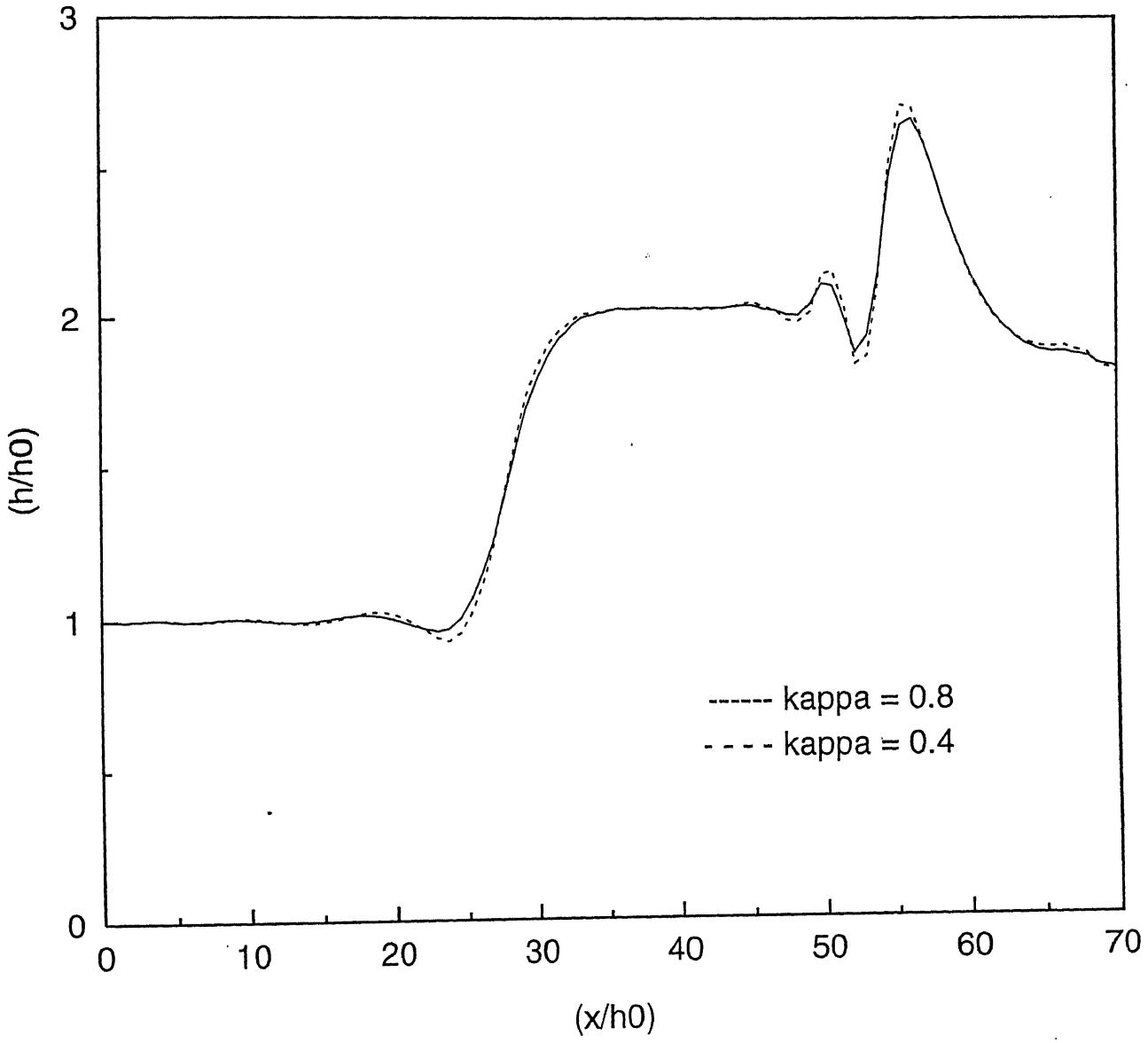

Fig 4.4 Effect of artificial viscosity

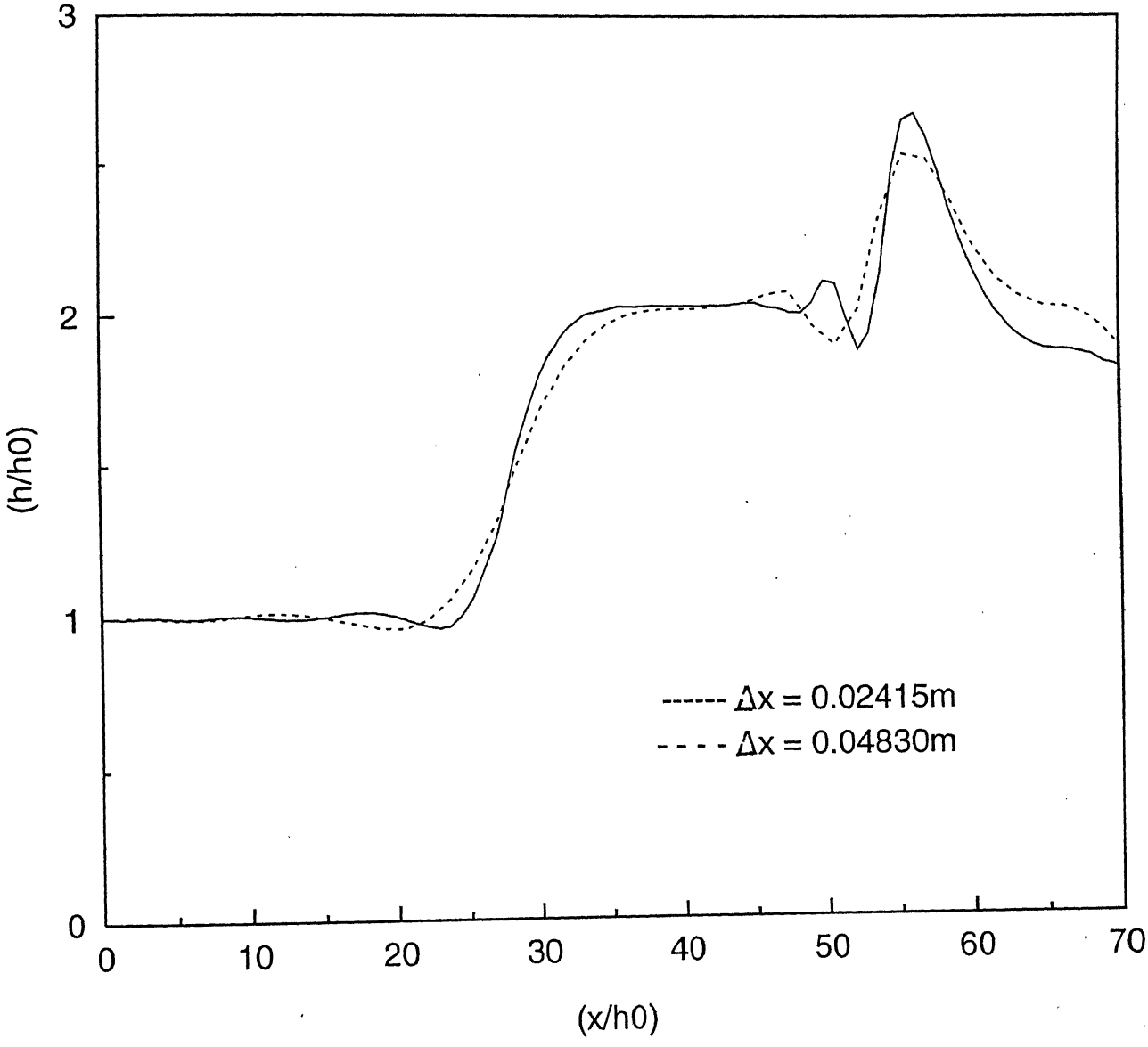

Fig 4.5 Effect of grid size

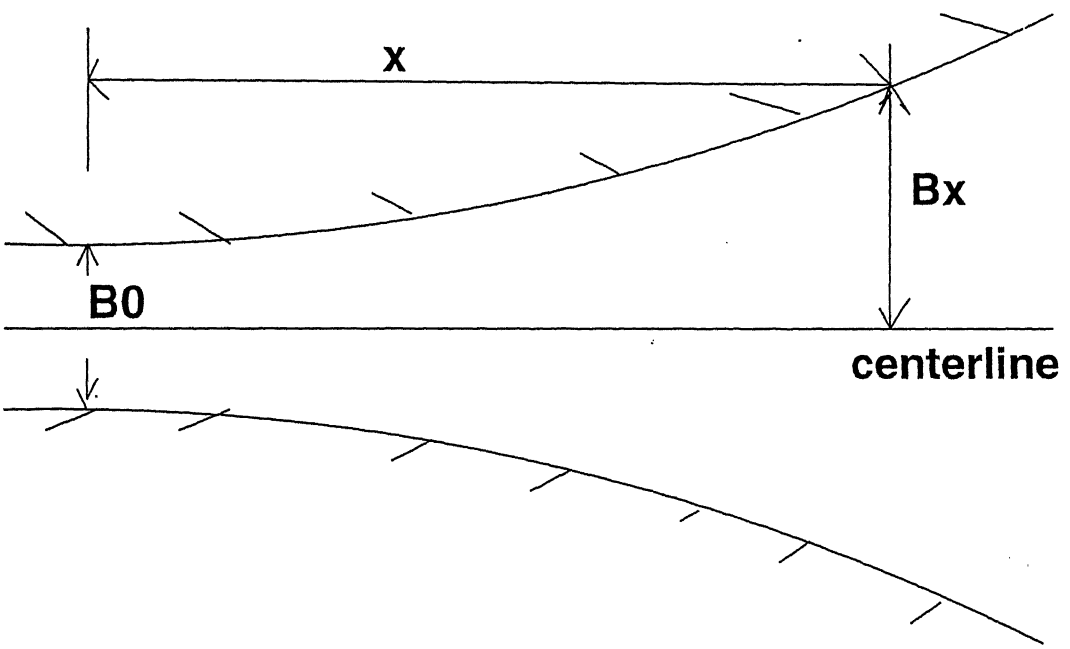

Fig 4.6 Gradual Expansion (Rouse et al. 1951)

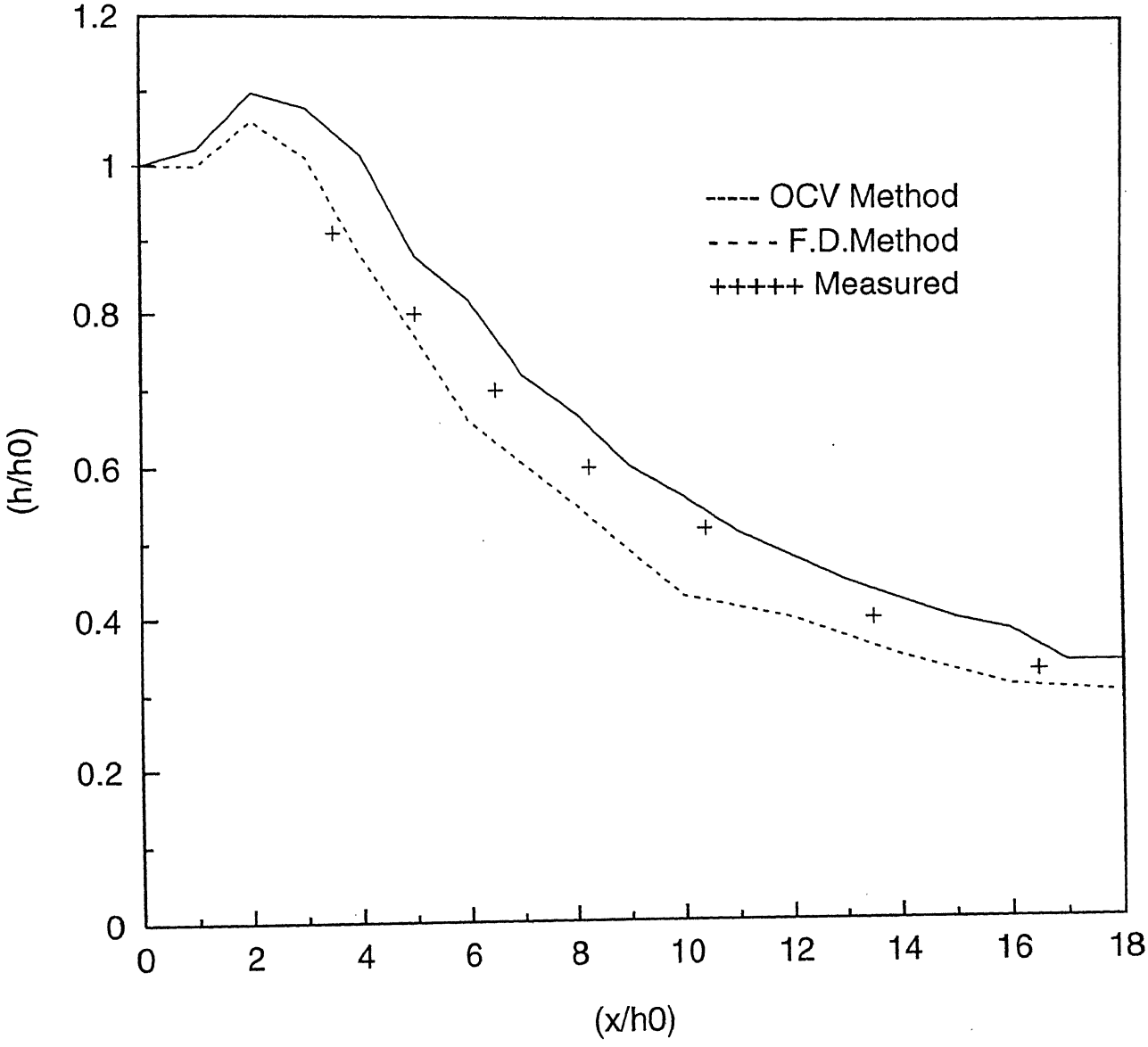

Fig 4.7 Water surface profile along the Centerline for expansion of fig 4.6

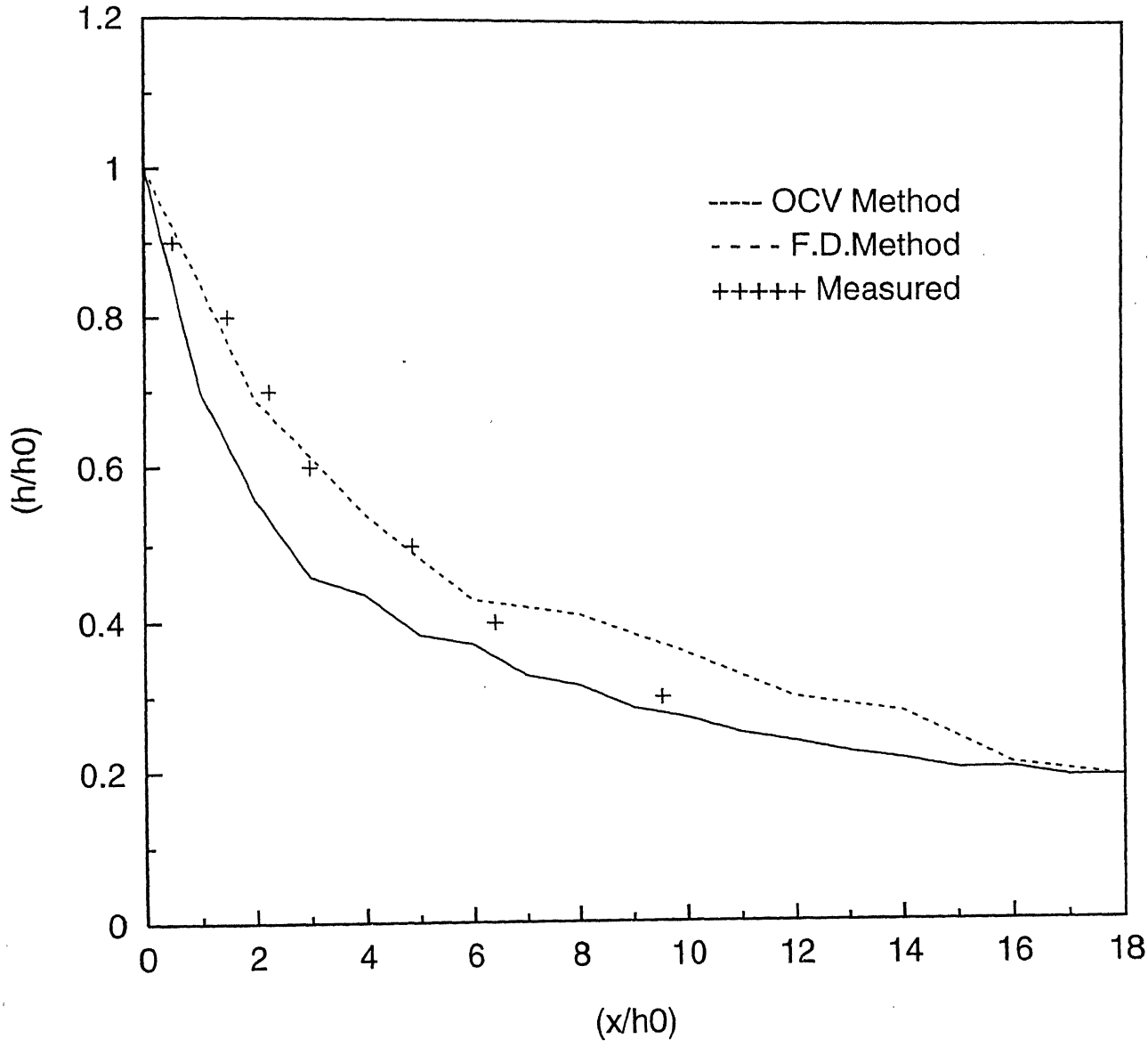

Fig 4.8 Water surface profile along the Wall for Expansion of Fig 4.6

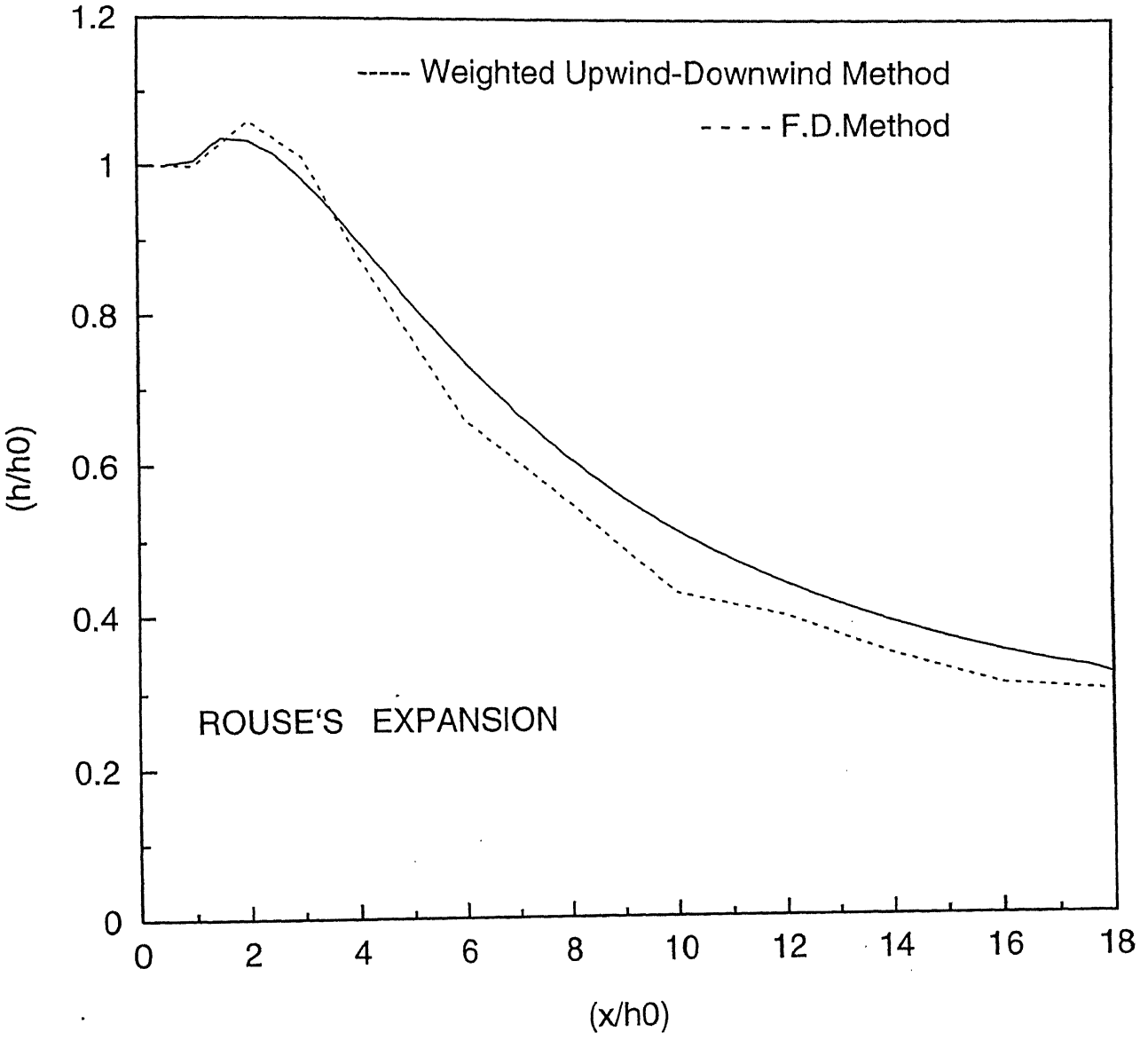

Fig 4.9 Water surface profile along the centerline

(Weighted Upwind-Downwind Method)

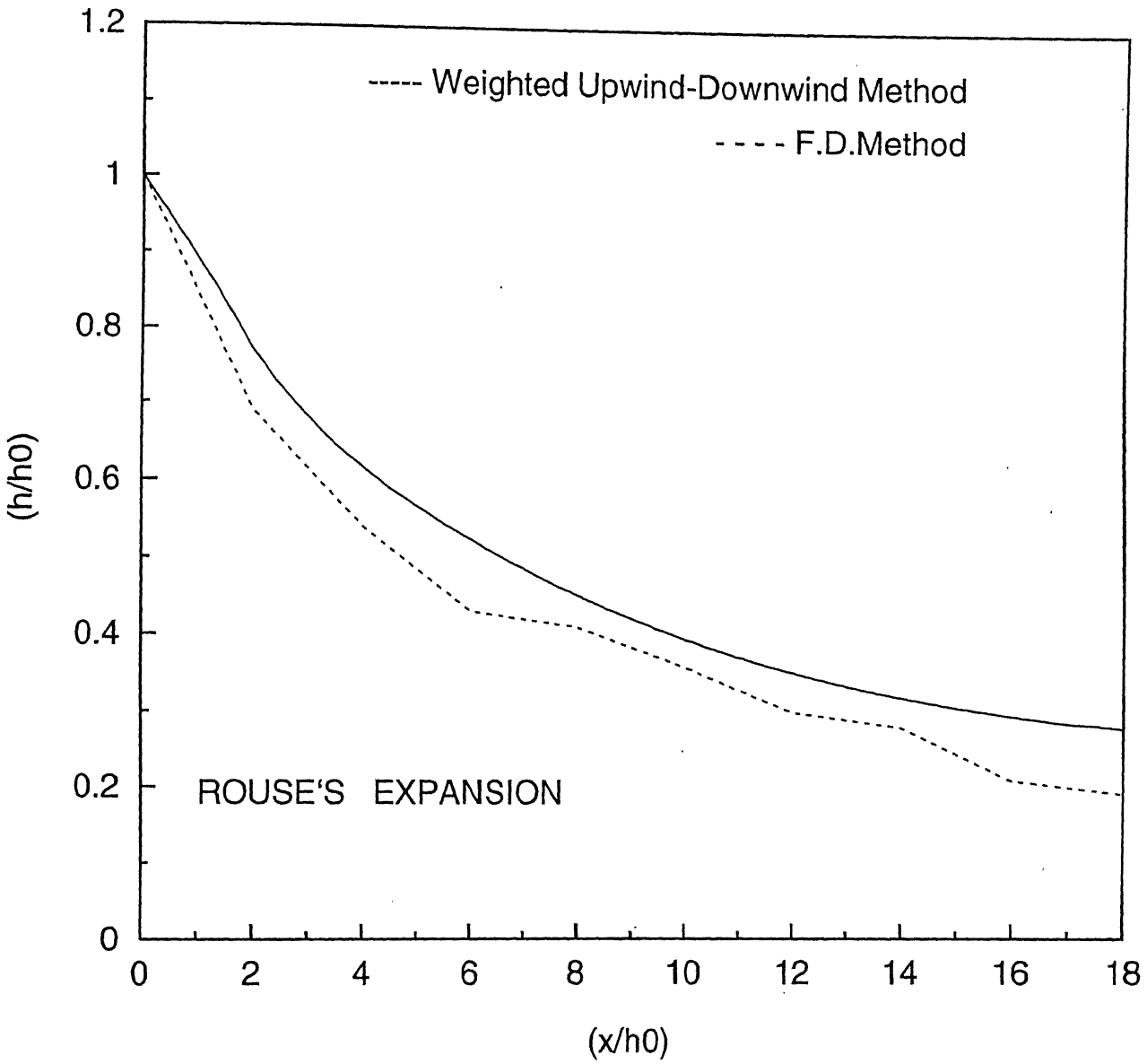

Fig 4.10 Water surface profile along the Wall

(Weighted Upwind-Downwind Method)

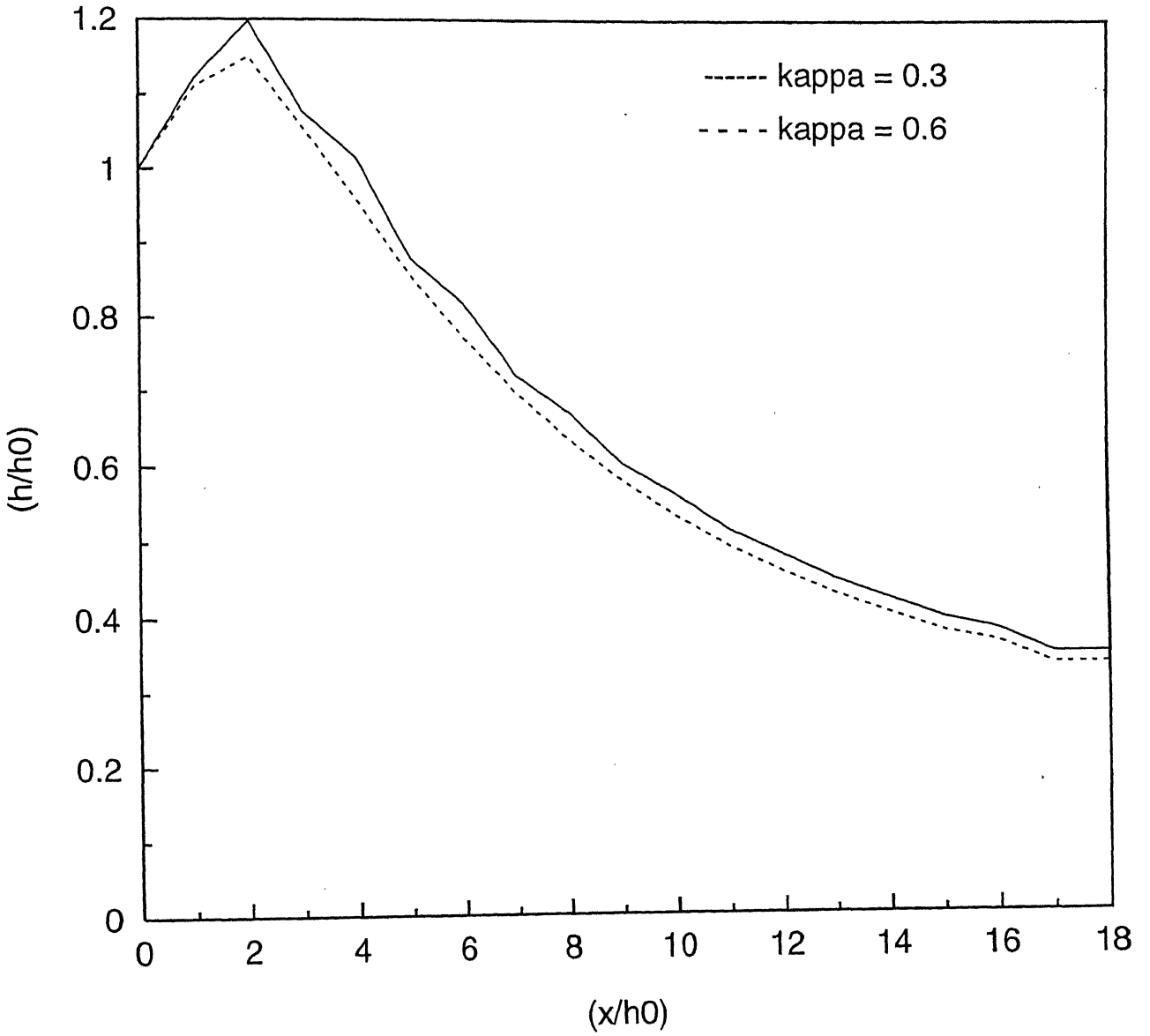

Fig 4.11 Effect of artificial viscosity for expansion problem (Centerline profile)

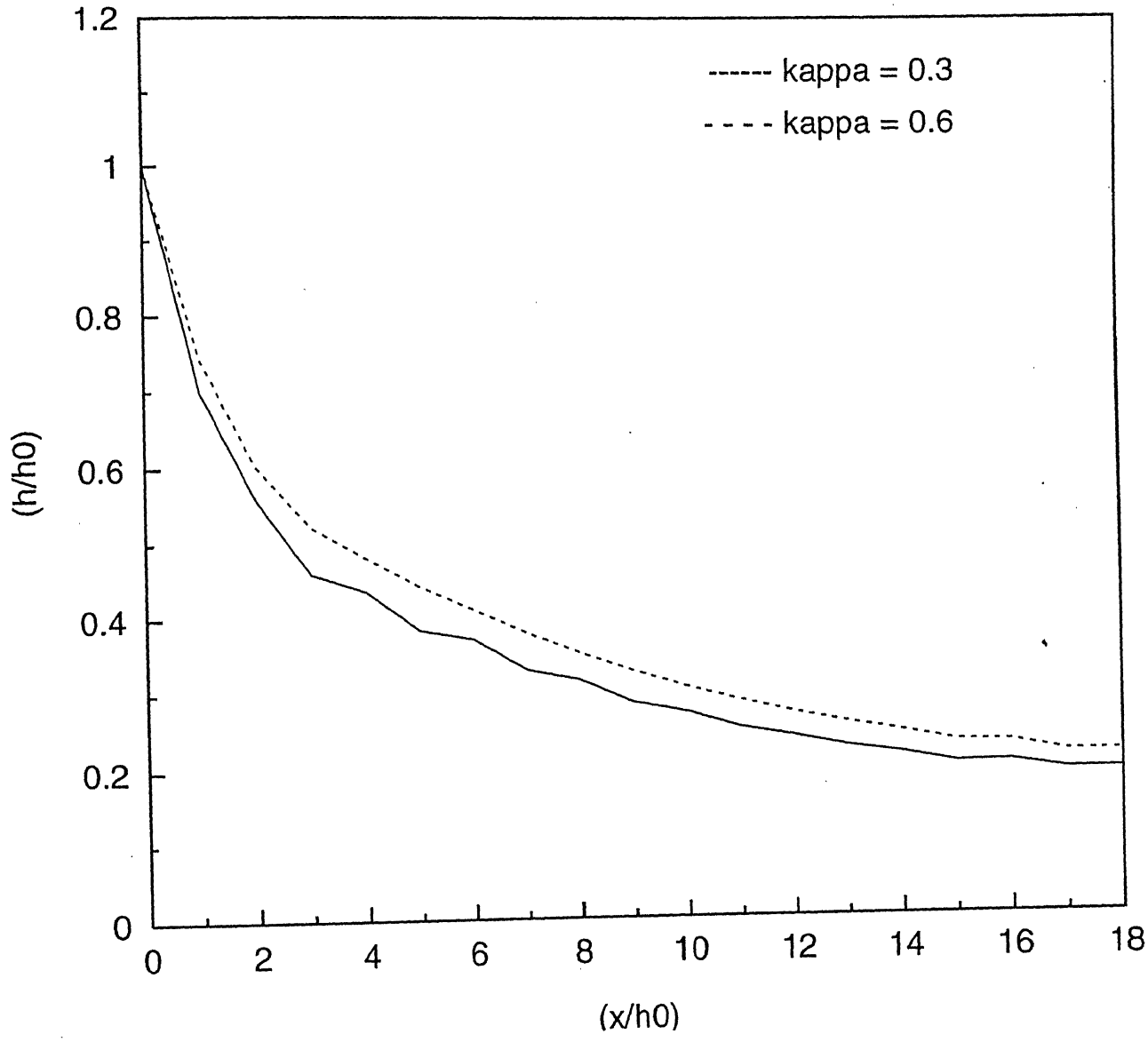

Fig 4.12 Effect of artificial viscosity for expansion problem (Wall profile)

Chapter 5

Summary and Conclusions

In this study, a control volume technique has been developed for solving the shallow water flow equations which describe the unsteady open–channel flows. The proposed control volume technique is based on the principle of overlapping control volumes suggested by Verma and Eswaran (1996) . The time discretization is done using a MacCormack type Predictor–Corrector approach. First–order upwinding and first–order downwinding are used for computing fluxes at the control surface during predictor and corrector calculations, respectively. The higher–order dispersive errors which result because of the second–order accuracy of the scheme are eliminated using the artificial viscosity approach. Alternatively, a weighted upwind–downwind method is proposed for this purpose.

The *OCV* technique has been applied for simulating the steady two–dimensional supercritical flows in channel transitions. The unsteady computations were used in a false–transient approach to obtain the steady state solutions. Both channel expansions and contractions were considered as test cases. The numerical results obtained using the *OCV* technique matched very well with the earlier numerical solutions obtained using the finite–difference approach. The numerical results also matched satisfactorily with the experimental data for those cases where the shallow water flow assumption is valid.

The main advantage of the proposed *OCV* technique is that it can be applied to general non–orthogonal domains without having to do the cumbersome coordinate

transformation. Unlike the finite–element techniques, it is easy to implement and the computational requirements are are not high. As compared to the usual finite–volume techniques, the proposed *OCV* technique uses the grid point coordinates, directly, to form the control volumes. It does not require the determination of the intermediate points for forming the control volumes.

The proposed weighted upwind–downwind method worked well for the case of channel expansions in which the water surface profile was smooth. However, it did not give correct results for the case of channel contractions in which shocks are present . *OCV* technique with artificial viscosity approach worked well for both the cases. However, artificial viscosity approach has been controversial in recent years since it uses an adjustable parameter. Further studies are required to incorporate the Total Variation Diminishing (TVD) principle into the *OCV* technique.

REFERENCES

Akanbi, A.A. and Katapodes, N.D. (1988) "Model for flood propagation on initially dry land" , Jour. of Amer. Soc. Civ. Engrs. , Vol.114, (7), pp689-706.

Alcrudo, F. Garcia–Novvarro, P. and Saviron, J.M. (1992) "Flux–difference splitting for 1-Dimensional open channel flow equations". Intl. Jour. for numerical methods in fluids, Vol 14, pp1009-1018.

Alcrudo, F. and Garcia, N.P. (1993) A TVD scheme in Finite–volumes for simulation of two–dimensional discontinuous flows. Intl. Jour. for Numerical Methods in Fluids. Vol.16, pp489-505.

Anderson, D.A., Tannehill, J.D. and Pletcher, R.H., (1984), *Computational Fluid Mechanics and Heat transfer*, McGraw-Hill,New York.

Bellos, C.V. , Soulis, J.V. and Sakkas, J.G. (1991) Computation of two–dimensional dambreak induced flows. Computational Mechanics Publications. *Advanced Water Res.* Vol.14, No.1 .

Bhallamudi, S.M. and Chaudhary, M.H., (1992), "Computation of flows in Open-Channel Transitions", Journal of Hydraulic Research, IAHR, Vol. 30, No.1, pp. 77-93.

Casulli, V. (1990), "Numerical Simulation of shallow water flow ", in Computational methods in Surface Hydrology, (Ed: Gambolti, G. et al.), Springer-Verlag.

Chaudhary, M.H. (1993), *Open-Channel Flow*, Prentice hall, New Jersey.

Chaudhary, M.H. , Bhallamudi, S.M. and Gharangik, A.M. (1985) em Mathematical modelling of flows in Baker Bay – Technical report prepared for U.S.Army Corpse of Engineers, Portland, Oregon.

Dammular, D. , Bhallamudi, S.M. and Chaudhry, M.H. (1989) Modelling of Unsteady flow in Curved channels, Jour. of Hydr. Engg., ASCE, 115 (11) ; 1479-95.

Fennema, R.J. and Chaudhry, M.H. (1989) Implicit methods for two–dimensional unsteady free surface flows, Jour. of Hydr. Res. , IAHR, 27(3) ; pp 321-32.

Fennema, R.J. and Chaudhry, M.H. (1990) Numerical Solution of Two–Dimensional Transient Free Surface Flows, Jour. of Hydr. Eng., Amer. Soc. Civ. Engrs., Vol 116, Aug., pp1013-1034.

Galland, J.C. et al. (1991) *TELEMAC*; A New Numerical Model for Solving Shallow Water Flow Equations. Adv. Water Res. Vol. 14, No.3 .

MacCormack, R.W., (1969). The Effect of viscosity in hypervelocity impact cratering, *Amer. Inst. Aeronautics and Astronautics*, Paper 69-354, Cincinnati, Ohio.

Nujic, M. (1995) Efficient implementation of non-oscillatory schemes for the computation of free-surface flows, IAHR, Vol.33, No.1, pp101-110.

Peyret, R. and Taylor, T.D. (1983) *Computational Methods for Fluid Flow*, Springer-Verlag, New York, 1983.

Puri, A.N. and Kao, C.Y., (1985), "Numerical Modelling of Subcritical Open Channel Flow Using The κ-ϵ Turbulence Model and The Penalty Function Finite Element Technique," Appl. Math. Modelling, vol. 9, No. 2, Apr., pp.82-88.

Putti, M , Yeh, W.W.G. and Mulder, W.A. (1990) 'A Tringular finite volume approach with high resolution upwind terms for the solution of ground water transport equation' , Water Res. Research, 26, pp2865-2880.

Roache, P.J., (1972), *Computational Fluid Dynamics*, Hermosa Publishers.

Rouse, H., Bhoota, B.V., and Hsu, E.Y. (1951). Design of channel espansions, Trans., Amer. Soc. Civil Engrs., 116:347 .

Savic, L.J. and Holly Jr., F.M. (1993) Dambreak flood waves computed by modified Godunov method. , IAHR, Vol.31 , No.2 , pp187-204.

U.S. Army Corpse of Engrs. (1985) "TABS-2 : User's Manual for the Generalized Computer program system, open channel flow and sedimentation" , Waterways Experiment Station, Vicksburg.

Verma, A.K , Eswaran, V. (1996) 'Overlapping Control Volume approach for convection-diffusion equation', Int. J. Numer. Methods in Fluids [in press].

Verma, A.K. , Bhallamudi, S.M. and Eswaran, V. (1996) 'Overlapping Control Volume Method for Solute Transport' Paper Communicated to Intl. Journal for Numer. Methods in Engg. .

Yang, J.Y. , Hsu, C.A. and Chang, S.H. (1993) Computation of free surface flows, Part 1 : One-dimensional dambreak flow, IAHR, Vol.31, pp19-34.